# Characterising the effect of Röntgen-radiation levels on germinating cress seeds by means of the biocrystallization method

Jelmer A. Zandbergen
Wageningen University
Registration nr: 921108982040
Supervisor: senior researcher Paul Doesburg, Crystal Lab, Ottersum
Date: 30-06-2014
Course, code: BSc Thesis Plant Sciences, YPS-82318

*Biocrystallization pattern of fresh cress (Lepidium sativum* L.*) extract*

# Content

# Preface

This research project was carried out in the final phase of my Bachelor's study Plant Sciences at Wageningen University in the Netherlands. The project forms an integral part of the study in which the acquired knowledge and skills come into practice. This study is conducted together with my supervisor, senior researcher Paul Doesburg from Crystal Lab in Ottersum, the Netherlands.
During my minor Sustainable International Agriculture in Witzenhausen, Germany, I followed a lecture by Dr. Jürgen Fritz who collaborates with Paul Doesburg on the biocrystallization method. This lecture was about this method and during the lecture I discovered that the biocrystallization method has a more holistic approach to the physiology of living organisms. There is currently a call for a more holistic approach within the field of life sciences, and this method could be used as a complementary method to broaden the prevailing reductionistic, materialistic scientific stance. Dr. Jürgen Fritz brought me into contact with Paul Doesburg, with whom I could join in a project, the FDK (Fremdkörperdetektion) project, on the influence of Röntgen radiation on germinating cress seeds.
I am interested in the more holistic approach, as I recognize living systems are more than just the sum of their parts. By conducting this research project with the obtained knowledge and skills in my previous study years I expect to contribute to the development of the biocrystallization method.
Within this thesis paper I give an introduction to the underlying mechanism of the formation of crystallization patterns, namely self-organization. This thermodynamic process is seen in all living systems and organisms in nature. Because within my study Plant Sciences I chose my major on cultivation and ecology, I will introduce the self-organization concept in relation to the science of ecology. Also I will introduce how this concept can be brought into practice in agriculture. I will further discuss the complementary value of the biocrystallization method to current research methodologies and why this method is applied with respect to the FKD (Fremdkörperdetektion) project.

# Abstract

Due to the prevailing reductionistic, materialistic, scientific stance organisms are perceived as merely built up out of single compounds. However, from different fields of science this concept is challenged by stating an organism is greater than the sum of its parts. A living organism or system has the ability to arrange its parts into a more ordered pattern by taking energy from outside itself and processing it to produce a more organized state, which is called self-organization. From the arisen organization, the system has gained properties that cannot be reduced to the properties of its constituting parts. In order to analyse such abilities, appropriate methods are needed at a more holistic level.

This study focused on a method, called the biocrystallization method, which has been used for decades as a holistic approach for quality assessment of agricultural products. For this method, a solution of dihydrate cupric chloride with an extract of cress seedlings as additive is allowed to crystallize under standardised conditions on a glass plate. Crystallization patterns emerge through the process of self-organization of dihydrate cupric chloride. The additive affects this self-organization process. In this research project the biocrystallization method was used to analyse the effects of Röntgen radiation on germinating cress seeds.

Röntgen radiation detection methods are used intensively in the evaluation of food products by the food industry. However, to what extent the food product itself, as a whole, is influenced by using Röntgen radiation detection methods has got only minor attention thus far. The biocrystallization method seems to reflect plant physiological processes, and it is on this level that a Röntgen radiation effect might be found and interpreted. In this project the biocrystallization method was used to detect whether Röntgen radiation affects the germination of cress (*Lepidium sativum* L.) as observed in the crystallization patterns.

Three experiments were carried out of which two experiments served as reference series, registering the effect of varying amounts of cress extract and degrees of decomposition of cress extract on the crystallization patterns. The third, main experiment was performed as a blind test determining whether varying levels of Röntgen radiation are reflected in the crystallization patterns. The varying levels included 50 mGy, 500 mGy, and a control group that was not radiated. The crystallization patterns were evaluated visually through a ranking test based on perceptual-learning under supervised categorisation. Besides, the patterns were analysed via computerized image analysis.

It was shown through visual evaluation that the treatment levels of Röntgen radiation could be significantly differentiated. The control seed batch had the lowest mean ranking score, the 50 mGy had the highest mean ranking score, and the 500 mGy radiated seeds had a mean ranking score in between. These observed effects complement earlier scientific findings on the effects of Röntgen radiation levels on plant physiology through hormesis. The image analysis results indicated differences in the distribution of needle lengths for both reference series, but the effect of Röntgen radiation could not be detected.

In order to better understand the crystallization pattern formation, further research can be aimed at studying whether plant physiological specific self-organization structures appear by observing the infrared spectra during heat convection in the dish.

# Introduction

## Introduction to self-organization

Reductionism is the prevailing scientific way of thinking which considers a living organism to be a complex set of atoms and molecules without considering its integrity (Looijen 2000). Atoms are thought to be the indivisible building blocks of nature according to the reductionistic theory (Baars and Baars 2007). This viewpoint contrasts to holism, which regards that parts of a whole have an intimate interconnection, such that they cannot exist independently of the whole. From this holistic stance an organism is regarded as greater than the sum of its parts (Looijen 2000). However, the ontological holistic approach is hardly accepted in agricultural sciences (Baars and Baars 2007). The controversy between a constructivist approach and an ontological holistic approach can be understood as a result of conflicting strategies in science by denying the value of each of both for specific realms in nature: the lifeless and the living. As is mentioned by Looijen (2000) the contrasting approaches should, however, be seen as mutually dependent. The consequence of the prevailing reductionistic approach is that there is little consideration for research methodologies that examine the integrity of organisms. The tenability of the reductionistic approach, however, can be questioned by examining the self-organizational ability of living organisms and systems in space and time.

Self-organization can be described as "the spontaneous creation of a globally coherent pattern out of local interactions" (Heylighen 2001). A living organism or system has the ability to arrange its parts into a more ordered pattern by taking energy from outside itself and processing it to produce a more organized state (Schneider and Kay 1995). From the arisen organization, the system has gained properties that cannot be reduced to the properties of its elements (Heylighen 2001).

According to Heylighen (2001), self-organization of a living organism, in thermodynamical terms, can be understood from the fact that a living system is considered an open system where energy and matter are flowing through. Entropy is continuously being created, but actively dissipated out of the system again. An open system moves therefore away from thermodynamic equilibrium, so having the ability to decrease its entropy at the expense of producing entropy in the larger system of which it is part. Self-organization is an effective process to reduce the external energy that impresses the system. Or in other words, self-organization makes dissipation more effective (Heylighen 2001).

## Self-organization in ecosystems

In the article of Schneider and Kay (1995) the earlier work of the re-examination of the rules of thermodynamics is continued. They show that the restated second law of thermodynamics is a fundamental principle within living systems as it underlies the direction of many processes observed in nature. In their article they focus on the application of the re-examination of the rules of thermodynamics to the science of ecology. Following the thermodynamic principles, the large gradient that the sun impresses on an ecosystem will be reduced in an ecosystem through the development of structures and functions that lead to a more effective dissipation of the solar energy. "As ecosystems develop or mature, they should increase their total dissipation, and should develop more complex structures with greater diversity and more hierarchical levels to abet energy degradation." (Schneider and Kay 1995) Succession of an ecosystem from this point of view is then seen as a result of the system organizing itself to dissipate more incoming energy with each stage of succession.

In a system perturbations occur as well. These can increase the entropy of a system again, moving the system towards thermodynamic equilibrium. When ecosystems get stressed by e.g. hurricanes, pest outbreaks, etc., they resemble earlier successional stages (Schneider and Kay 1995). In order to make a system more resilient against such perturbations, a system needs a variety of regulatory mechanisms (Heylighen 2001). DNA can be seen as such a regulatory mechanism (Schneider and Kay 1995). It may be considered a memorising agent for the dissipating structure of the concerning organism. The gradient dissipating processes are then allowed to continue without the dependency on stochastic events (Schneider and Kay 1995).

Besides the resilience against perturbations of regulatory mechanisms, simultaneously these regulatory mechanisms resist the system to be moved further from thermodynamic equilibrium. "In any real system there is an upper limit to the gradient which can be applied to the system." (Schneider and Kay 1995) Therefore, without any perturbations, a system may end up in a local minimum stable state where it will not be able to switch to an alternative stable state (Scheffer, Carpenter et al. 2001). Indeterminism that is being created by perturbations, e.g. hurricanes, pest outbreaks, fires, etc., can help a system to escape a local minimum stable state, enabling the system to reach a stable state that may be even further away from thermodynamic equilibrium (Heylighen 2001). However, there is a risk that such events may also enable the system to reach an equilibrium state that is closer to thermodynamic equilibrium (Scheffer, Carpenter et al. 2001). Consequently, in a living system there should be a balance of regulatory mechanisms that maintain order, and perturbations that disturb the system (Heylighen 2001).
According to Scheffer, Carpenter et al. (2001), maintaining resilience should currently be the main focus of sustainable management, so implementing regulatory mechanisms in a system. There is an increasing interest for systems that apply self-regulation (Napel ten, Bianchi et al. 2006). Ten Napel, Bianchi et al. (2006) mention the need for another view on maintaining balance on agricultural systems by minimizing the impact of perturbations on the system instead of aiming for keeping disturbances away, by applying self-regulating processes. Examples of self-regulating processes on agricultural level can be integrated pest management strategies. Also sustaining or developing landscape complexity can be a strategy to enhance self-regulation. A hypothesized model by Tscharntke, Bommarco et al. (2007) shows that the recovery ability of any disturbance on native natural enemies, which have the ability to control biological processes, is higher for more complex, or heterogeneous, landscapes than for more homogeneous landscapes. Moreover, homogeneous landscapes even have the tendency to not fully recover at all, meaning a decrease in biological control over time and thus a decrease in the self-regulating capacity. As a consequence of that, the system is more susceptible to perturbations that cause to system to be brought closer to thermodynamic equilibrium (Scheffer, Carpenter et al. 2001).
Ten Napel, Bianchi et al. (2006) and Lammerts van Bueren, Struik et al. (2002) mention that the self-regulating capacity of an agricultural system is one of the key aspects of organic agriculture. In order to achieve self-regulation and thus maintaining balance, Ten Napel, Bianchi et al. (2006) calls for the need of robust varieties. In the paper of Lammerts van Bueren, Struik et al. (2002), it is mentioned that such traits are not yet included in breeding programmes, but are needed to further optimize the self-regulation principle of organic farming systems. Such optimization increases the resilience of a system, and makes it consequently harder for a perturbation to switch the system to an alternative state (Scheffer, Carpenter et al. 2001).
When the system gets disturbed, regulatory mechanisms will be activated in order to maintain its homeostasis (Calabrese and Baldwin 2002). This accounts for living systems as well as individual organisms. But in order to directly analyse how homeostasis of living organisms is affected by physiological processes as a result of perturbations in its environment, a method is needed that can actually analyse such effects. Such a method would be based on a more holistic stance, as it does not focus on the regulatory mechanisms of the system, but on how the system's homeostasis is influenced as a whole, and reacts.

## Introduction to the biocrystallization method

Baars and Baars (2007) mention the need for more holistic concepts. What is seen in such concepts, however, is that scientific validation is needed in order not to end up in a vague conceptual context (Huber, Bloksma et al. 2006). The Louis Bolk Institute has developed and validated such a concept, the Inner Quality concept. The Inner Quality concept is based on plant physiological processes during the vegetative phase (growth) and the generative phase (differentiation), and the integration between the two processes (Northolt, van der Burgt et al. 2004). Only a few methods seem appropriate to measure Inner Quality, of which the biocrystallization method is one (Kahl, van der Burgt et al. 2010).
The biocrystallization method is used for decades as a holistic approach for quality assessment of agricultural products. It uses a solution of dihydrate cupric chloride with an organic extract as additive. This substance is allowed to crystallise under standardised conditions on a glass plate.

Two-dimensional dendritic patterns emerge through the process of self-organization of dihydrate cupric chloride (Busscher, Kahl et al. 2014). Extracts from different (industrial treated) agricultural products are chosen. "The emerging patterns reflect physiological processes like maturation and decomposition, the effect of processing, feeding regime and production system in a broad range of agricultural products." (Doesburg and Nierop 2013) In the paper of Fritz, Athmann et al., (2011) three image analysis methods, amongst which the biocrystallization method, were used to analyse wheat samples from different agricultural production systems. The images were typical and reproducible and could be successfully grouped and assigned to the respective agricultural production system (Bio-dynamic, Bio-organic, Integrated, Integrated no manure, unfertilized), indicating a good reliability of the biocrystallization method.
How the mechanism of the formation of crystallization patterns exactly works is still being investigated (Busscher, Kahl et al. 2014). The general mechanism behind crystallization pattern formation is an entropy exporting system (Kahl, Bodroza-Solarov et al. 2013). Because of a temperature gradient impressing the glass plate system in the crystallization chamber, the process of self-organization takes place in order to dissipate this gradient. The randomly moving molecules in the glass plate system become fixed by passing on the energy of their movement to the liquid in which they are dissolved. So, the liquid effectively increases in entropy and the crystal itself decreases in entropy (Heylighen 2001). This results in two-dimensional dendritic growth. The branching conditions change when a food sample in the form of a juice or extract is added to the solution (Kahl, Bodroza-Solarov et al. 2013), and the crystallization patterns are additive-specific (Andersen, Henriksen et al. 1999). Because the crystallization process is highly sensitive to environmental conditions, climatic standardisation measures are important. Standardisation measures influence the repeatability of the crystallization patterns, which is essential for statistical analysis and grouping of patterns from different treatments.
The emerging patterns are evaluated visually (Huber, Andersen et al. 2010, Fritz, Athmann et al. 2011), or by computerized evaluation methods (Andersen, Henriksen et al. 1999, Doesburg and Nierop 2013). Scientific research demands objective data acquisition methods, whereby human's subjectiveness in an experimental setting is being eliminated (Looijen 2000). In order for the visual evaluation to be standardised and validated Huber, Andersen et al. (2010) have developed a method to visually analyse crystallization patterns on a more objective manner. According to several criteria a biocrystallization pattern is evaluated. "These criteria have been defined and references are available in connection to a scale. All this is performed by consensus, according to an adapted ISO-norm for sensory evaluation." (Huber, Andersen et al. 2010). With this development the biocrystallization method has a more fundamental scientifically accepted and communicable base and an essential step is taken (Huber, Andersen et al. 2010).

## Application of the biocrystallization method to the FKD project

For this research project, the biocrystallization method is used to detect whether Röntgen radiation as used in Röntgen-detection analysis has an effect on germinating cress seeds. This project is part of the FKD (Fremdkörperdetektion)–project, initiated by the Forschungsring für Biologisch-Dynamische Wirtschaftsweise e.V. as a response to the increasing use of Röntgen radiation detection methods in the food industry (LomaSystems 2013). Röntgen radiation detection methods are used in order to detect whether contaminants, e.g. plastic, glass particles, are located in food products. For a food processing company, a recall of the order may be the consequence of such a discovery. Moreover, its brand and success may be affected when their client finds out impurities in the food (LomaSystems 2013). In order to avoid consequences like these and to assure a company's security norms, precaution measures like Röntgen radiation detection methods can be advantageous (LomaSystems 2013). 35 out of the 40 largest food-processing companies make use of Röntgen detection methods in 100 countries around the world (LomaSystems 2013). With the intensive and expected increasing use of Röntgen radiation detection methods for food products, it is necessary to evaluate the effect of such treatments on the food product itself.
The leading question within the FKD project is whether Röntgen radiation practices influence food quality. In this context, quality is considered from both an ontological reductionistic (the product's constituents), and a holistic stance. With respect to the latter, the biocrystallization method seems to reflect plant physiological processes (Kahl, van der Burgt et al. 2010), and it is on this level that

Röntgen radiation effects might be found and interpreted. In this project the biocrystallization method is used to analyse whether radiation originating from Röntgen detection methods has an effect on germinating cress seeds (*Lepidium sativum* L.). The hypothesis is that effects can indeed be found as observed in the crystallization patterns. This hypothesis is based on earlier scientific work on the effects of Röntgen radiation on homeostasis (Calabrese and Baldwin 2002) and the ontological holistic approach of the biocrystallization method. The found crystallization effects will be considered and discussed with respect to the available literature on Röntgen radiation effects on homeostasis.

# Materials and methods

## General information

For this research project, three experiments were carried out in the laboratory of senior researcher Paul Doesburg, Crystal Lab, Ottersum (NL). The first two experiments served as reference series, consisting of an additive reference series and a decomposition reference series. The goal of the additive reference series is to characterize the Gestalt-domain 'Additive dominance'. For the decomposition reference series, the goal is to characterize the Gestalt-domain 'Decomposition'. A Gestalt is defined as "a perceptual pattern or structure possessing qualities as a whole that cannot be described merely as a sum of its parts" (CollinsEnglishDictionary 2014) which complies more closely to the pattern-formation principle of the method than a mere morphological characterization. These characterizations are used to both get familiar with the cress-specific crystallization pattern (additive reference series) and to interpret the crystallization patterns from the third, Röntgen radiation experiment (decomposition reference series).

## Seed selection

For the experiments, cress seeds (*Lepidium sativum* L. Bingenheimer Saatgut AG, Echzell-Bingenheim, Germany, article no. G250, Kresse Einfache) were used. The seeds were selected based on mechanical size (circular sieve 1.5-1.75mm). Further selection was conducted on density fractionation, and a subsequent visual/manual selection based on the following 3 overall features: size (very small/large seeds were discarded), colour (very light-brown/dark-brown seeds were discarded; seeds with spots and mis-colouring were discarded) and morphological features (broken, damaged, irregularly shaped and insufficiently filled seeds were discarded). These selection criteria were used in order to acquire uniform stock material, so as to minimize the effect of variability of non-relevant features.

## Seed germination

Seed germination during the experiments took place on chromatography paper (blotting paper 151B; 85 × 140 mm; 87 g/m2; thickness 0.17 mm; Frisenette, Knebel, Denmark), placed in plastic bags (Zipper bag, transparent, 100 x 150 mm, 50µm LDPE). 3.00 ml of demineralised water was pipetted onto the paper and when the water was absorbed evenly over the paper, 16 seeds were placed on the paper. A total of 10 bags were applied per treatment in order to acquire 3 grams of seedlings per treatment. Seed samples of the treatments were germinated in two-fold repetitions per experiment. The bags were placed in a germination box and this box was placed in a heating cabinet at 18$^{o}$C (+/- 1$^{o}$C). After 2.5 hours, the cress seeds formed a mucous layer. They were aligned 9 cm from the bottom of the chromatography paper, approximately 2mm apart. The bags were placed back in the germination box in the heating cabinet for another 93.5 hours (+/- 0.5h) (attachment 1, figure 25, 26, 27).

## Seedling extraction and preparation crystallization solution

After the germination, an extraction of the seedlings was carried out (Baumgartner, Doesburg et al. 2012). From every treatment 3 grams of seedlings were selected exhibiting a minimal root-length of 6.5 cm, wetted with 10 ml of demineralised water, and then crushed by means of a pestle for 3 minutes, after which no intact leaf or root parts were observed in the solution. Subsequently, another 17 ml of water was added to get a 10% extraction solution. The extract solutions were then placed on a horizontal shaker at 125 rpm for 45 min. The extract was then filtered by means of a nylon filter with pore-size 150 µm, in order for the fluid to remain. This filtering step decreases the amount of cress by filtering out the larger, and insoluble parts.
To this filtered extract, originating from the 10% watery cress solution, a solution of cupric chloride (Baumgartner, Doesburg et al. 2012) was added (for specific solutions for the experiments see sections below). Every combination of extract and a solution of cupric chloride is called a chamber solution, as this substrate will be pipetted on the glass plates (1st quality float glass; "air side" applied; 100.0mm diameter; thickness 2.0 mm ± 0.2; Pfaehler GmbH & Co. KG, Gengenbach,

Germany) in the crystallization chamber. In order to create a basin for pipetting the chamber solution, an acrylic ring (made from GS acrylic tubes Riacryl; length 35 mm, thickness 5 mm ± 0.5 mm; Broennum Plast, Rodovre, Denmark) was added using Vaseline (Prolabo, Fontenay sous Bois, France; article no. 28 908.290) as adhesive material (Baumgartner, Doesburg et al. 2012). A 6.0 ml volume of the chamber solution was pipetted on the glass plates. For every chamber solution one portion of 6 ml was made in addition, because of the errors made during pipetting. The glass plates were assigned to pre-specified positions in the crystallization chamber. In the crystallization chamber there are 43 positions. For every crystallization procedure, all positions have to be occupied in order to attain a standardized microenvironment for each experimental procedure. In these experiments carrot juice (pasteurized, commercially available in local food store) was used as additive to $CuCl_2.2H_2O$ for filling the remaining positions.

## Crystallization chamber specifications

The chamber is held on a temperature of 30$^{o}$C below the glass plates. Outside the crystallization chamber, the temperature is kept constant at 25,7$^{o}$C and the relative humidity is kept constant at 44%. Consequently, the relative humidity inside the crystallization chamber is constant as well. Because of the different microenvironment inside the crystallization chamber, there is a temperature and humidity gradient influencing the crystallization process. These settings are based on standard freeze-dried wheat, such that the mean initial nucleation time of the crystallization patterns is 12h ± 1 h (will be explained further). The freeze-dried wheat extract – $CuCl_2$ mixing ratio used for the standardization was 90 mg of extract and 90 mg of $CuCl_2$ per glass plate (Busscher, Kahl et al. 2010).

## Visual and computerized evaluation of crystallization patterns

After the crystallization process is completed, the plates are taken out and scanned (after a min. 24h drying period) using a PowerLook III UMAX Scanner at 600 dpi (Busscher, Kahl et al. 2010). Eventually the crystallization patterns are evaluated by visual evaluation and by computerized image analysis. For the visual evaluation, the crystallization patterns were grouped according to a comparable initial nucleation time. This procedure is carried out, because the initial nucleation time influences the morphology of the crystallized patterns. In order to obtain meaningful differences of the patterns due to the treatments only, without the influence of initial nucleation time, this step is an essential one. The initial nucleation time is registered through a camera making pictures every 10 min of each glass plate in the crystallization chamber. The moment when the $CuCl_2.2H_2O$ starts to crystallize is denoted as the initial nucleation time. The time until completion of the crystallization pattern is not denoted, because this is hard to observe from the pictures that are made from each glass plate during the crystallization procedure.

For the visual evaluation of the crystallization patterns obtained from each experiment, a list was made of relevant features characterizing the treatments as reflected in the crystallization patterns. These features were defined according to the nomenclature of Huber, Andersen et al. (2010) for characterizing crystallization patterns. Their relevant differences were defined according to three categories of evaluation criteria in concordance with Huber, Andersen et al. (2010): (1) Quantifiable single morphological and local features, (2) Quantifiable, descriptive single morphological features, (3) Gestures or implicit motions in the whole pattern.

Besides, for the two reference series, the sensed "activity" between the crystallization patterns was defined through perceptual learning under supervised categorization (Ashby and Maddox 2005, Galotti 2013) in order to obtain a more profound perception of the dynamics between the treatments.

Computerized structure image analysis was also performed. This analysis calculates the count of needle fragments of 15 structural analysis length-variables. The parameter L20 represents a maximum length of 2 pixels, L26 represents a length between 2 and 2.6 pixels, likewise for L33, L41, L51, L62, L75, L89, L108, L124, L144, L167, L192, L220, ending with L250 representing all lengths exceeding 22 pixels (Doesburg and Nierop 2013). Analysis was performed on different regions of interest (ROIs) of the crystallization patterns in order to obtain information on where differences in needle length may be located. The ROI is a restricted circular area of the biocrystallization pattern (figure 1). In the experiments the ROI 0-30% (relative to the geometrical centre of the glass plate), 0-50%, 0-70%, 0-90%, 50-70%, and 70-90% were used.
Statistical analysis on the obtained data was performed with IBM SPSS v. 19.0.

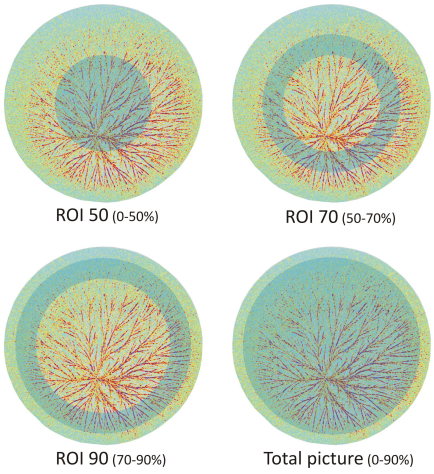


Figure 1: An example of different regions of interest of a crystallization pattern. ROI (region of interest) is a restricted circular area of the biocrystallization pattern.

## Additive reference series specifications

With the additive experiment (general set-up, attachment 2) a reference series was obtained reflecting the effects of varying amounts of cress extract on the resulting crystallization pattern. For this, increasing amounts of cress additive were used, obtained from a filtered 10% watery extract, as described above. The amounts ranged from 200 to 400 mg of cress extract per glass plate at 50 mg intervals. This was mixed with 150 mg $CuCl_2.2H_2O$ from a 10% aqueous solution (henceforth denoted as 200-150, 250-150, etc.) (table 1).

Table 1: Chamber solutions specifications, Additive reference series

| | contents per plate | | | | | amounts needed (ml) | | |
|---|---|---|---|---|---|---|---|---|
| Chamber sol. # | cress (mg) | CuCl2 (mg) | volume (ml) | plate replicates | portions | watery cress extract | CuCl2 | H2O |
| 1 | 200.00 | 150.00 | 6.00 | 10 | 11 | 22.00 | 16.50 | 27.50 |
| 2 | 250.00 | 150.00 | 6.00 | 9 | 10 | 25.00 | 15.00 | 20.00 |
| 3 | 300.00 | 150.00 | 6.00 | 8 | 9 | 27.00 | 13.50 | 13.50 |
| 4 | 350.00 | 150.00 | 6.00 | 8 | 9 | 31.50 | 13.50 | 9.00 |
| 5 | 400.00 | 150.00 | 6.00 | 8 | 9 | 36.00 | 13.50 | 4.50 |

## Decomposition reference series specifications

The decomposition experiment (general set-up, attachment 3) resulted in another reference series in order to interpret the crystallization patterns from the third, Röntgen radiation experiment. In this experiment filtered 10% watery cress extracts, as described above, decomposed for 0 (fresh extract), 1, 2, 3 and 4 days were used as additive to a 10% $CuCl_2.2H_2O$ solution at a mixing ratio of 300 mg cress extract and 150 mg $CuCl_2.2H_2O$ (table 2). The chamber solutions were allowed to decompose by storing them in an Erlenmeyer sealed with Parafilm at 4°C. For each treatment 6 glass plates were pipetted resulting in 30 glass plates in total. The remaining positions were filled with glass plates with carrot juice as additive to $CuCl_2.2H_2O$, as mentioned above.

Table 2: Chamber solutions specifications, Decomposition reference series

| | | contents per plate | | | | | amounts needed (ml) | | |
|---|---|---|---|---|---|---|---|---|---|
| Chamber sol. # | treatment | substance (mg) | CuCl2 (mg) | volume (ml) | plate replicates | portions | substance | CuCl2 | H2O |
| 1 | fresh cress extract | 300.00 | 150.00 | 6.00 | 6 | 7 | 21.00 | 10.50 | 10.50 |
| 2 | 1 day decomp. | 300.00 | 150.00 | 6.00 | 6 | 7 | 21.00 | 10.50 | 10.50 |
| 3 | 2 days decomp. | 300.00 | 150.00 | 6.00 | 6 | 7 | 21.00 | 10.50 | 10.50 |
| 4 | 3 days decomp. | 300.00 | 150.00 | 6.00 | 6 | 7 | 21.00 | 10.50 | 10.50 |
| 5 | 4 days decomp. | 300.00 | 150.00 | 6.00 | 6 | 7 | 21.00 | 10.50 | 10.50 |
| 6 | carrot juice | 190.00 | 150.00 | 6.00 | 13 | 15 | 2.85 | 22.50 | 64.65 |

For the decomposition series a ranking exam was performed. This was done so as to statistically analyse whether the different decomposition treatments as reflected in the crystallization patterns could be differentiated visually. For this, crystallization patterns were photographed from the fresh, one day decomposed, and three days decomposed extract. Patterns were grouped according to a comparable initial nucleation time. The series of images were coded and a panel of two observers independently from each other observed all series. The crystallization patterns were ranked according to the degree of perceived decomposition from 1 (fewest 'Decomposition' features) to 3 (most 'Decomposition' features) according to the features characterizing the Gestalt 'Decomposition'.

## Röntgen radiation experiment specifications

During the third, main experiment (general set-up, attachment 4) cress seeds were used that were subjected to Röntgen-radiation with two different intensities. In order for the seeds to be sensitive enough, the cress seeds were wetted (2% $H_2O$) for 3.5 hours before radiation. After the radiation treatment, they were dried back for 24 hours at room temperature (20°C, 45% humidity). Radiation was conducted by using an X-ray tube, Titan Isovolt 160 E from the company GE Measurement & Control.
Three groups of equally large seed batches were formed. One that is not radiated to serve as control group, one treated with 50 mGy and one treated with 500 mGy (table 3). In order to filter out the lower-energy photons emitted by the tube before reaching the target, one thin aluminium plate was used. After the radiation treatment, the seed batches were randomized and coded (A, B, and C). The Röntgen radiation treatment was performed at the TU in Darmstadt (Germany), after which the coded seed batches were sent to the laboratory.

Table 3: Röntgen tube (Titan Isovolt 160 E, GE Measurement & Control) settings applied to realize the two radiation levels.

| Radiation dose (mGy) | Voltage (kV) | Amperage (mA) | Time (s) | Distance from the source (cm) |
|---|---|---|---|---|
| 500 | 90 | 19 | 13 | 30 |
| 50 | 90 | 19 | 11 | 72 |

This experiment was performed in three repetitions, and for each experiment an alternating processing order for each treatment A, B, and C, was conducted so as to minimize the effect of processing order on the final results (Baumgartner, Doesburg et al. 2012). After the seed germination, seedling analysis was performed on the root length and root weight. These measures served as a complementary physiological analysis to the results from the biocrystallization procedure. A picture was made from each bag of seedlings (attachment 1, figure 25, 26, 27). From these pictures the length of all seedling roots was determined using the Image-J plugin *Smartroot* (Lobet, Pages et al. 2011). Before extraction of the seedlings, from the selected seedlings from each filter the mean seedling-weight was determined.
A mixing ratio of 150 mg $CuCl_2.2H_2O$ (5% aqueous solution) and 300 mg filtered 10% watery cress extract was used for every treatment (table 4). Per treatment a total of 6 glass plates was pipetted, resulting in 18 glass plates for the three treatments. For each experiment the treatments were repeated twice, resulting in a total of 12 glass plates per treatment and 36 glass plates in total for the experiment. The remaining positions were filled with glass plates with carrot juice extract as additive, as mentioned above.

Table 4: Chamber solutions specifications, Röntgen radiation experiment

| | | contents per plate | | | | | amounts needed (ml) | | |
|---|---|---|---|---|---|---|---|---|---|
| Chamber sol. # | treatment | substance (mg) | CuCl2 (mg) | volume (ml) | plate replicates | portions | substance | CuCl2 | H2O |
| 1 | A | 300.00 | 150.00 | 6.00 | 6 | 7 | 21.00 | 21.00 | 0.00 |
| 2 | B | 300.00 | 150.00 | 6.00 | 6 | 7 | 21.00 | 21.00 | 0.00 |
| 3 | C | 300.00 | 150.00 | 6.00 | 6 | 7 | 21.00 | 21.00 | 0.00 |
| 4 | C | 300.00 | 150.00 | 6.00 | 6 | 7 | 21.00 | 21.00 | 0.00 |
| 5 | B | 300.00 | 150.00 | 6.00 | 6 | 7 | 21.00 | 21.00 | 0.00 |
| 6 | A | 300.00 | 150.00 | 6.00 | 6 | 7 | 21.00 | 21.00 | 0.00 |
| 7 | carrot juice | 190.00 | 150.00 | 6.00 | 7 | 10 | 1.90 | 30.00 | 28.10 |

For this experiment, a ranking test was performed in order to statistically analyse whether a differentiation between the treatments could be found. Prior to the visual evaluation ranking test, the relevant features as reflected in the crystallization patterns were defined during a process of perceptual-learning under supervised categorisation (Ashby and Maddox 2005, Galotti 2013). Hereby, the Gestalt-domain 'Decomposition' was used obtained from the decomposition reference series. The coded treatments were assigned into groups according to this Gestalt-domain and other relevant features as reflected in the crystallization patterns.
For the visual evaluation ranking test, a total of 25 series consisting of the crystallization patterns of the three treatments was obtained. For this, a discrete number of patterns (N=13) was used creating the multiple series. The series were coded and randomized for the visual evaluation. Visual evaluation was conducted by a panel of two evaluators. The crystallization patterns within each series were scored from 1 to 3, based on the results of the perceptual-learning under supervised categorisation.

# Results

## Additive reference series

Analysis of the chamber performance does not indicate that there were major differences in initial nucleation time caused by environmental deviations during the crystallization procedure. The mean of the crystallization nucleation time of all treatments from this reference series is 14.37 hrs. with a standard deviation of 1.223 hrs. The mean nucleation time of the individual treatments (6 measurements per treatment) does not show a tendency to deviate from the overall mean (N=5*6=30) (figure 1).

From the patterns derived from the different additive ratios, features that characterize their relevant differences were defined (table 5).
The activity that was sensed in the biocrystallization patterns with increasing ratios of cress extract is defined as (figure 2-6):

- A simultaneous occurring expansion towards the periphery and cress-specific differentiation with fullness, Beweglichkeit and 'vitality'.

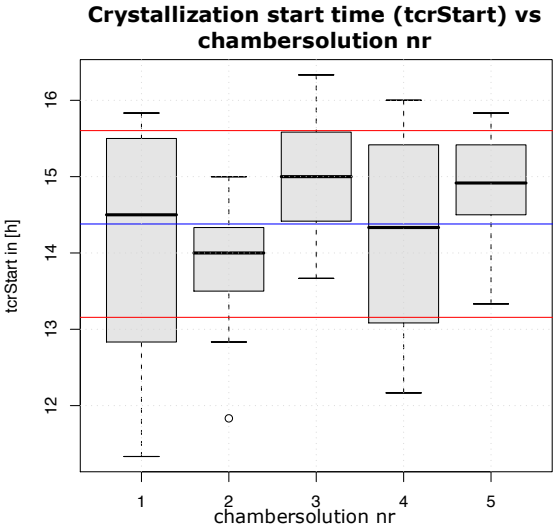


Figure 1: Boxplot view showing the deviation from the overall mean (14.37 hrs., N=30) of the initial nucleation time (tcrStart) of each individual chamber solution (N=6) of the substance additive reference series. Chamber solution nr 1 is mixing ratio 200-150, nr 2 is 250-150, etc. It appears that all distributions have a mean within the range of 1 sd unit (1.223 hrs.) from the overall mean.

Table 5: Features characterizing the influence of increasing additive-ratios as reflected in cress biocrystallization patterns. Nomenclature according to Huber, Andersen et al. (2010).

| Quantifiable single morphological and local features | Quantifiable, descriptive single morphological features | Gestures or implicit motions in the whole pattern |
|---|---|---|
| Decrease of coarse structural features | Decrease of Dense radial formations | Increase of Integration |
| Increase of Fullness of sideneedles | Decrease of Thining-out | Increase of Beweglichkeit |
| | Increase of Clear stems | Increase of Durchstrahlung |

Figure 2: Biocrystallization pattern with a mixing ratio of 200 mg cress extract and 150 mg CuCl2

Figure 3: Biocrystallization pattern with a mixing ratio of 250 mg cress extract and 150 mg CuCl2

Figure 4: Biocrystallization pattern with a mixing ratio of 300 mg cress extract and 150 mg CuCl2

Figure 5: Biocrystallization pattern with a mixing ratio of 350 mg cress extract and 150 mg CuCl2

Figure 6: Biocrystallization pattern with a mixing ratio of 400 mg cress extract and 150 mg CuCl2

The response of the structure image analysis was parameter depended. The needle fragment distributions reflected a decrease of smaller crystal fragments, with increasing additive ratio at ROI 0-90%. This difference is to a lesser extent found in ROI 0-30%. From the comparison between ROI 50-70% and ROI 70-90% it is seen that the differences are higher in the region of 50-70% of the pattern (figure 7).
The opposite accounts for longer needle fragments (figure 8). It is seen from ROI 0-90% that longer needle fragments are more abundant in the crystallization patterns of a higher extract ratios. This difference is not found in ROI 0-50% and lower. By comparing ROI 50-70% and ROI 70-90% the difference is mainly found in ROI 70-90%, meaning that longer needle fragments are higher in number in ROI 70-90%.

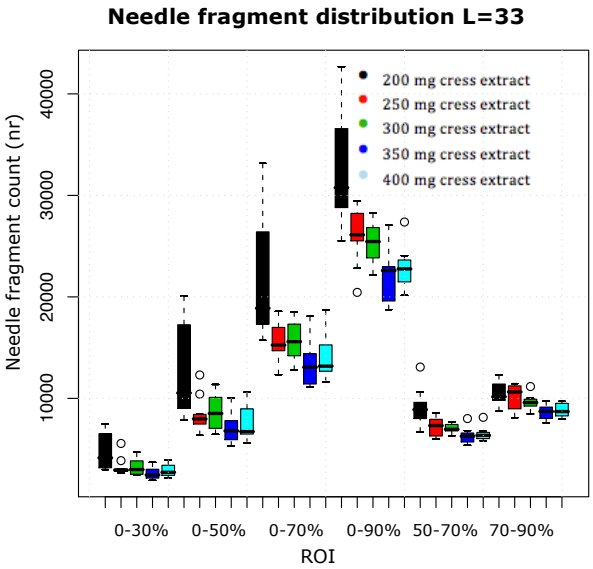


Figure 7: Distribution of number of fragments of needle length L=33 for additive mixing ratios ranging from 200 mg to 400 mg cress extract with 50 mg intervals. Distributions are shown for each measured ROI. ROI analysed: 0-30% until 0-90%, and 50-70% and 70-90%.

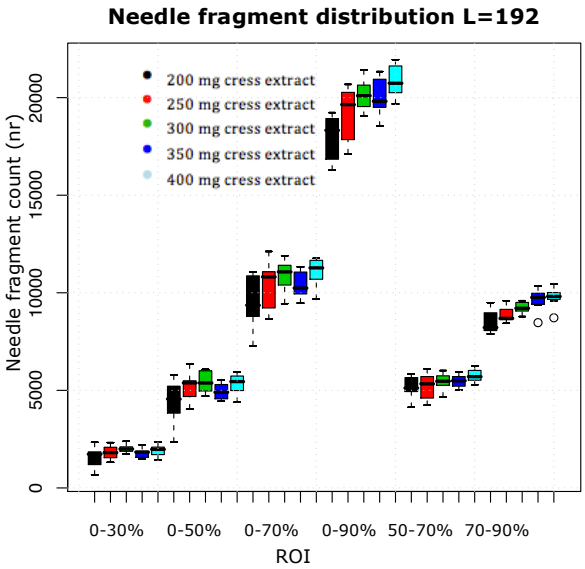


Figure 8: Distribution of number of fragments of needle length L=192 for additive mixing ratios ranging from 200 mg to 400 mg cress extract with 50 mg intervals. Distributions are shown for each measured ROI. ROI analysed: 0-30% until 0-90%, and 50-70% and 70-90%.

## Decomposition reference series

Concerning the analysis of the chamber performance of the crystal patterns of the decomposition reference series, it is seen just as from the Additive reference series that there is no indication that differences in the crystal patterns may have been caused by environmental factors. The mean of the crystal nucleation time is 13.16 hrs. with a standard deviation of 1.108. The individual treatment means (6 measurements per treatment) seem not to deviate from the overall mean (N=6*6=36) (Figure 9).

The relevant differences between the crystallization patterns derived from the different decomposition steps were defined (table 6).
The activity perceived in the biocrystallization patterns of increasingly decomposed cress extract is defined as (figure 10,11,12):

- The compression into increasingly rigid, coarse structures, loss of differentiation of fine structures.

The needle-coverage decreases with increasing decomposition and loses regularity in the progression from the centre to the periphery.

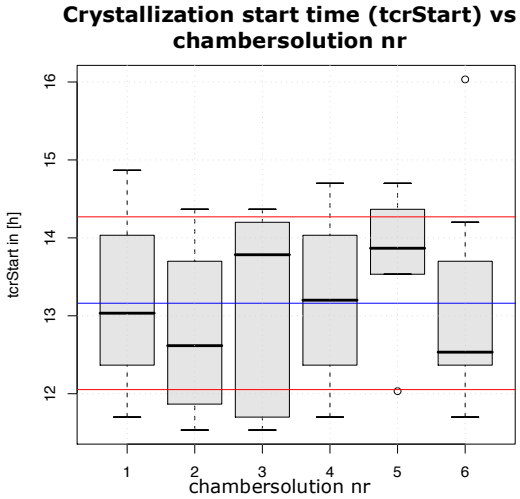


Figure 9: Boxplot view showing the deviation from the overall mean (13.16 hrs., N=36) of the initial nucleation time (tcrStart) of each individual chamber solution (N=6) of the decomposition reference series. Chamber solution nr 1: fresh extract; 2-5: respectively 1-4d decomposed extract; 6: carrot juice. It appears that all distributions have a mean within the range of 1 sd unit (1.108) from the overall mean.

Table 6: Features characterizing increased 'Decomposition' as reflected in cress biocrystallization patterns. Nomenclature according to Huber, Andersen et al. (2010).

| Quantifiable single morphological and local features | Quantifiable, descriptive single morphological features | Gestures or implicit motions in the whole pattern |
|---|---|---|
| • Increase of coarse structural features | • Increase of Flechtwerke | • Decrease of Integration |
| • Increase of the angle of ramification | • Increase of Thining-out | |
| | • Increase of Clear stems | |
| | • Decrease of Regularity of ramifications | |

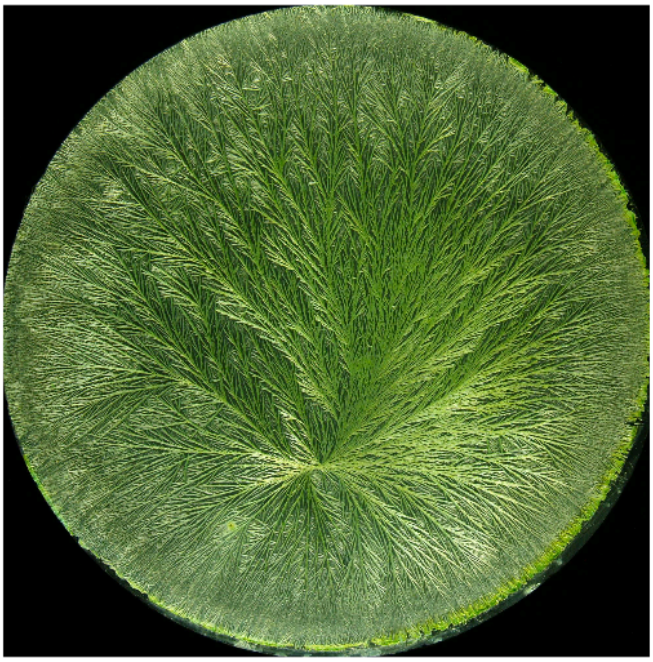

Figure 10: Biocrystallization pattern of a of fresh cress extract.

Figure 11: Biocrystallization pattern of a 1 day decomposed cress extract.

Figure 12: Biocrystallization pattern of a 3 days decomposed cress extract.

For the statistical analysis of the visual evaluation of the biocrystallization patterns of the three treatments, fresh, one day decomposed, and three days decomposed the mean ranking score of the biocrystallization patterns is represented in table 7. Statistical analysis has shown (table 8) that the mean ranking score of the biocrystallization patterns from the three extracts, fresh, one day decomposed and three days decomposed, is significantly (α=0.05) different among all groups (p=0.000). It is assumed that there is no observer effect, p=1.000. These results show that visual evaluation succeeded in assigning the biocrystallization patterns of the decomposition treatments in the right order.

Table 7: Descriptive statistics output for the mean ranking scores per treatment, and mean ranking scores of each observer.

**Dependent Variable: Score**

| Treatment | Observer | Mean | Std. Deviation | N |
|---|---|---|---|---|
| fresh | JZ | 1.2000 | .42164 | 10 |
| | PD | 1.1000 | .31623 | 10 |
| | Total | 1.1500 | .36635 | 20 |
| 1 day | JZ | 1.8000 | .42164 | 10 |
| | PD | 2.1000 | .56765 | 10 |
| | Total | 1.9500 | .51042 | 20 |
| 3 day | JZ | 3.0000 | .00000 | 10 |
| | PD | 2.8000 | .42164 | 10 |
| | Total | 2.9000 | .30779 | 20 |
| Total | JZ | 2.0000 | .83045 | 30 |
| | PD | 2.0000 | .83045 | 30 |
| | Total | 2.0000 | .82339 | 60 |

Table 8: Pairwise comparisons output for the analysis of mean ranking score differences between the treatments. For the mean ranking scores of the patterns, it is significantly (α=0.05) shown that all treatments are different from each other (p=0.000).

**Dependent Variable: Score**

| (I) Treatment | (J) Treatment | Mean Difference (I-J) | Std. Error | Sig.[b] | 95% Confidence Interval for Difference[b] | |
|---|---|---|---|---|---|---|
| | | | | | Lower Bound | Upper Bound |
| fresh | 1 day | -.800* | .129 | .000 | -1.058 | -.542 |
| | 3 day | -1.750* | .129 | .000 | -2.008 | -1.492 |
| 1 day | 3 day | -.950* | .129 | .000 | -1.208 | -.692 |
| | fresh | .800* | .129 | .000 | .542 | 1.058 |
| 3 day | 1 day | .950* | .129 | .000 | .692 | 1.208 |
| | fresh | 1.750* | .129 | .000 | 1.492 | 2.008 |

**Based on estimated marginal means**

***. The mean difference is significant at the 0.05 level.**

**b. Adjustment for multiple comparisons: Least Significant Difference (equivalent to no adjustments).**

Structure image analysis showed a parameter dependent response. The distributions of parameter L26 (figure 13) show that the four days decomposed extract has the highest number of fragments of all treatments. This accounts for all analysed ROIs. For the fresh extract, it is shown that the number of fragments is the lowest. Apart from the three days decomposed extract, the other treatments follow the trend of an increasing number of fragments with increasing decomposition time. It seems that the three days decomposed extract has lower values than expected. Furthermore, the differences between the treatments tend to get higher towards an increased ROI.
For length variable L160 (figure 14), all treatments appear to have an equal number of fragments along all analysed ROI.
When analysing variable L≥250 (figure 15), it seems that the distributions are exact the opposite from parameter L26. The four days decomposed extract has the lowest number of fragments of all treatments. This observation accounts again for all analysed ROIs. The differences seem to increase towards an increased ROI, which is equivalent to the distributions of parameter L26. Also within the parameter L≥250 the three days decomposed extract seems to defy the expected trend. It shows higher values than the trend would suggest.
The distributions of needle length fragments show differences at low (L26) and high (L≥250) needle length parameters, but opposite from each other. There are no differences found in the intermediate needle length parameter (L160).

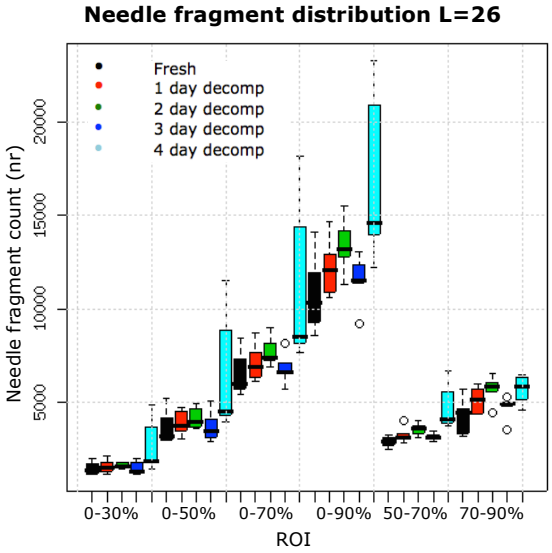


Figure 13: Distribution of fragments of length of short needles, L=26, per ROI of each series of decomposition treatments. ROI analysed: 0-30% until 0-90%, and 50-70% and 70-90%.

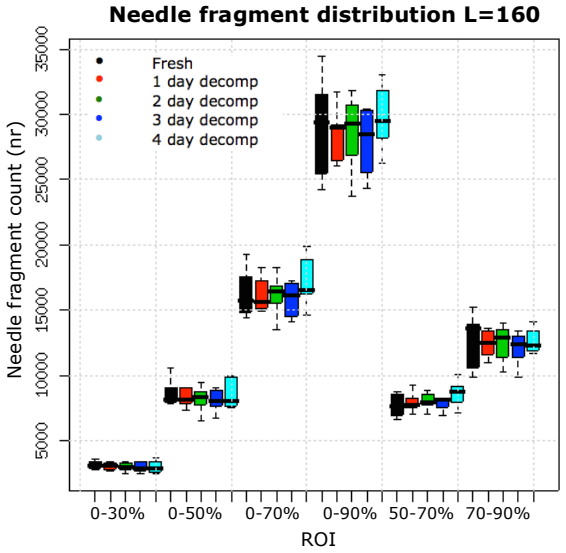


Figure 14: Distribution of fragments of middle length needles, L=106, per ROI of each series of decomposition treatments. ROI analysed: 0-30% until 0-90%, and 50-70% and 70-90%.

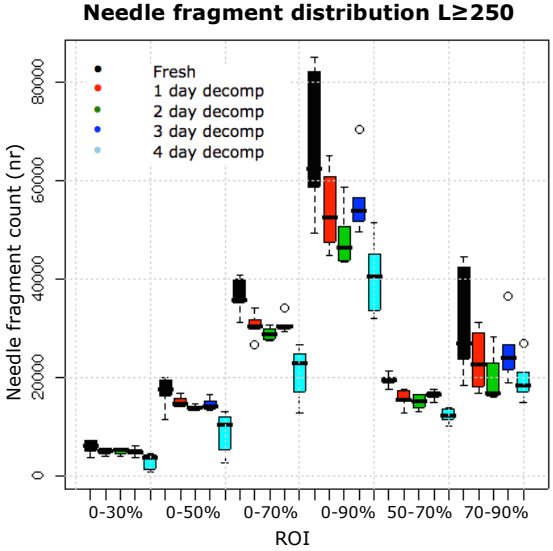


Figure 15: Distribution of fragments of long needle length, L≥250, per ROI of each series of decomposition treatments. ROI analysed: 0-30% until 0-90%, and 50-70% and 70-90%.

## Röntgen radiation experiment

From the decoding table (table 9) it is seen that treatment A had a radiation dose of 500 mGy, treatment B had a radiation dose of 50 mGy, and treatment C was the control group of which the seeds were not radiated, but only wetted and back-dried.

Table 9: Decoding table of the cress seed Röntgen radiation treatments A, B, and C and their matching dose, 500 mGy, 50 mGy, and control, respectively.

| Code | Radiation dose | sample | Ammount (g) | Radiation date |
|---|---|---|---|---|
| A | 500 mGy | Cress seed | 6,0 | 11.03.2014 |
| B | 50 mGy | Cress seed | 6,0 | 11.03.2014 |
| C | control | Cress seed | 6,0 | 11.03.2014 |

Analysis of the root length distribution of all germinated cress seedlings shows that the mean of the 50 mGy treatment (table 10) is significantly higher than the mean of the control group (p=0.011, table 12) and the 500 mGy treatment (p=0.015, table 12). It is not shown that the means of the control group and the 500 mGy treatment were significantly different (table 12).
From the calculated average seedling weight per bag there was no significant difference between the treatments observed in our analysis (data not shown). However, the seedlings of the 50 mGy treatment do have the tendency to have a higher mean weight than the seedlings of the 500 mGy treatment and the control group (table 11).

Table 10: Descriptive statistics output for the mean root length of cress seedlings per treatment and their associated standard deviation. The mean root length of treatment B (50 mGy) is higher than the mean root lengths of treatment A (500 mGy) and C (control).

Dependent Variable: Root_length

| Treatment | Mean | Std. Deviation | N |
|---|---|---|---|
| a | 5.696273 | 1.7386664 | 1241 |
| b | 5.863204 | 1.6982058 | 1261 |
| c | 5.688885 | 1.7107688 | 1251 |
| Total | 5.749899 | 1.7172938 | 3753 |

Table 11: Descriptive statistics output for the mean of average cress seedling weight per bag per treatment. Treatment B (50 mGy) appears to have a larger mean than treatment A (500 mGy) and C (control), however not significant ($\alpha = 0.05$) (data not shown).

Dependent Variable: Weight

| Treatment | Mean | Std. Deviation | N |
|---|---|---|---|
| a | .0326162 | .00143126 | 77 |
| b | .0329935 | .00135654 | 77 |
| c | .0327818 | .00125884 | 74 |
| Total | .0327974 | .00135492 | 228 |

Table 12: Pairwise comparison output for the mean difference in root length between the treatments and their associated standard error. Treatment B (50 mGy) shows a significantly ($\alpha = 0.05$) higher mean root length compared to treatment A (500 mGy) and C (control). Between treatment A (500 mGy) and C (control) there is no significant difference.

Dependent Variable: Root_length

| (I) Treatment | | Mean Difference (I-J) | Std. Error | Sig.[b] | Difference[b] Lower Bound | Difference[b] Upper Bound |
|---|---|---|---|---|---|---|
| a | b | -,167* | .069 | .015 | -.301 | -.032 |
| | c | .007 | .069 | .914 | -.127 | .142 |
| b | a | ,167* | .069 | .015 | .032 | .301 |
| | c | ,174* | .068 | .011 | .040 | .309 |
| c | a | -.007 | .069 | .914 | -.142 | .127 |
| | b | -,174* | .068 | .011 | -.309 | -.040 |

Based on estimated marginal means

*. The mean difference is significant at the .05 level.

b. Adjustment for multiple comparisons: Least Significant Difference (equivalent to no adjustments).

For the first main experiment performed on the 7th of April 2014, the mean initial nucleation time of all crystallization patterns was 14.43 hrs. (N=43) with a standard deviation of 1.385 hrs. The distributions of each individual chamber solution (N=6 for chamber solution 1 – 6, N=7 for chamber solutioin 7) do not show a deviation from the overall mean (figure 16).

The second main experiment was performed on the 14th of April 2014. The mean crystallization time was 14.15 (N=43) with a standard deviation of 1.541. From the individual chamber solution (N=6 for chamber solution 1 – 6, N=7 for chamber solutioin 7) distributions it appears that the crystallization patterns of chamber solution 3 and 6 deviate from the overall mean (figure 17). The other chamber solutions resulted in crystallization patterns that were within the range of the mean initial nucleation time and 1 sd unit.

On the 21st of April 2014 the third main experiment was conducted. The initial nucleation time has a mean of 13.13 hrs. (N=43) with a standard deviation of 1.354 hrs. The distributions of the initial nucleation times of each individual chamber solution (N=6 for chamber solution 1 – 6, N=7 for chamber solutioin 7) do not show to deviate from the overall mean initial nucleation time (figure 18).

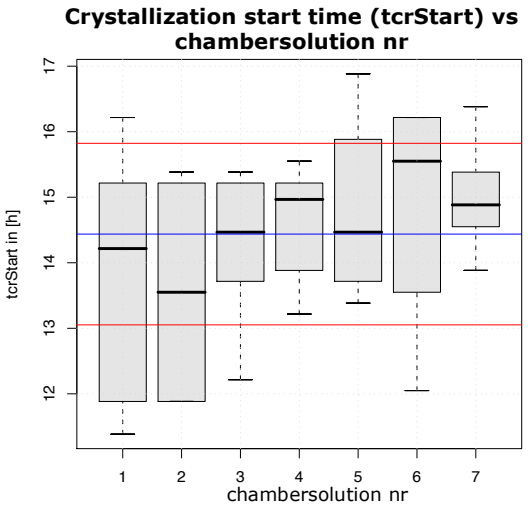


Figure 16: Boxplot view showing the deviation from the overall mean of the initial nucleation time of each individual chamber solution of the first main experiment. Chamber solution nr 1, 6: treatment A (500 mGy); nr 2, 5: treatment B (50 mGy); nr 3, 4: treatment C (control); nr 7: carrot juice.

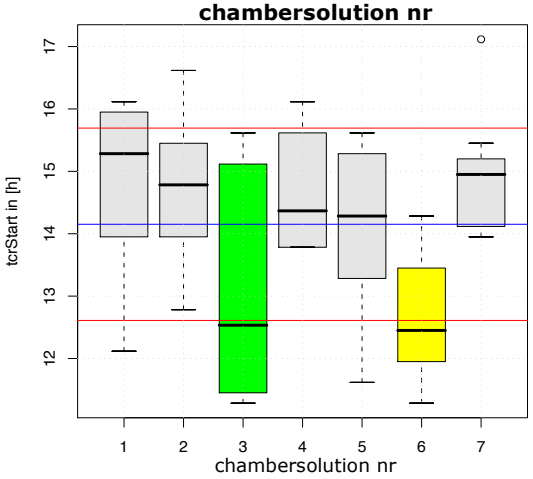


Figure 17: Boxplot view showing the deviation from the overall mean of the initial nucleation time of each individual chamber solution of the second main experiment. Chamber solution nr 1, 6: treatment B (50 mGy); nr 2, 5: treatment C (control); nr 3,4: treatment A (500 mGy); nr 7: carrot juice.

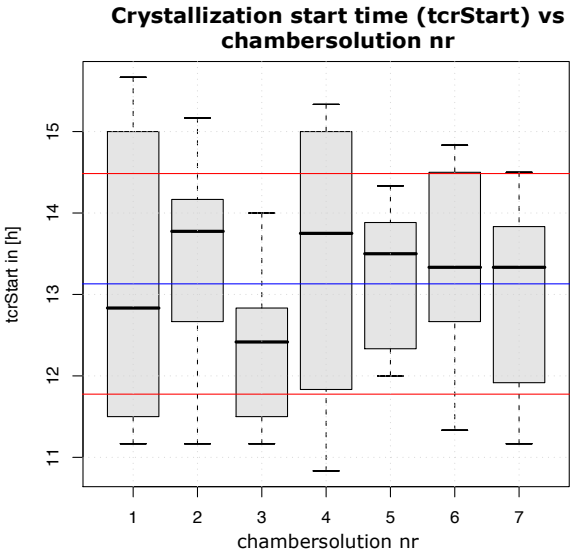


Figure 18: Boxplot view showing the deviation from the overall mean of the initial nucleation time of each individual chamber solution of the third main experiment. Chamber solution nr 1, 6: treatment C (control); nr 2, 5: treatment A (500 mGy); nr 3, 4: treatment B (50 mGy); nr 7: carrot juice.

Prior to the visual evaluation results, the result of the perceptual-learning under supervised categorisation was examined first. The result showed that the crystallization patterns of the 50 mGy treatment had both characteristics of a 'Decomposition' pattern, as shown in the decomposition reference series, and a more chaotic structure than the 500 mGy treatment and the control group. Scoring the crystallization patterns on either 'Decomposition' or chaotic features alone, however, did not succeed in categorizing the treatments. It appeared that the crystallization patterns of the control group had the fewest 'Decomposition' characteristics and showed the fewest chaotic features. The crystallization patterns from the 500 mGy treatment also showed both 'Decomposition' features and a chaotic structure to a certain degree, but less than the 50 mGy treatment did. From this, the scores 1 to 3 were defined as score 1 to be the crystallization pattern with the fewest 'Decomposition' and chaotic features until score 3 to be the crystallization pattern with the most 'Decomposition' and chaotic features.

From the visual evaluation scores of the 25 series (figure 20, 21, 22), the 50 mGy treatment has a mean ranking score of 2.36, the 500 mGy treatment has a mean ranking score of 2.00, and the control group has a mean ranking score of 1.64 (table 13). It is assumed that there are no significant ($\alpha$=0.05) differences among the observers (p=1.000) (table 14). All treatments are shown to be significantly different from each other ($\alpha$=0.05) (table 15). It is shown that the 50 mGy treatment has a significantly higher mean ranking score than the 500 mGy treatment (p=0.021) and the control group (p=0.000), and the 500 mGy treatment has a significantly higher mean than the control group (p=0.021) (table 13, figure 19).

The computerized image analysis was not able to detect clear differences in distributions of needle lengths among the different treatments (data not shown).

Table 13: Descriptive statistics table showing the mean ranking score of each treatment, and ranking scores per observer. Treatment A is 500 mGy, treatment B is 50 mGy, and treatment C is the control group.

Dependent Variable: Score

| Treatment | | Mean | Std. Deviation | N |
|---|---|---|---|---|
| a | JZ | 1.9600 | .93452 | 25 |
| | PD | 2.0400 | .84063 | 25 |
| | Total | 2.0000 | .88063 | 50 |
| b | JZ | 2.3600 | .70000 | 25 |
| | PD | 2.3600 | .81035 | 25 |
| | Total | 2.3600 | .74942 | 50 |
| c | JZ | 1.6800 | .69041 | 25 |
| | PD | 1.6000 | .64550 | 25 |
| | Total | 1.6400 | .66271 | 50 |
| Total | JZ | 2.0000 | .82199 | 75 |
| | PD | 2.0000 | .82199 | 75 |
| | Total | 2.0000 | .81923 | 150 |

Table 14: ANOVA table showing that there are significant differences in the mean treatment scores of the visual evaluation (F=10.869; p=0.000). It is not shown ($\alpha$=0.05) that there are differences in treatment scores among the observers (p=1.000).

Dependent Variable: Score

| Source | Type III Sum of Squares | df | Mean Square | F | Sig. |
|---|---|---|---|---|---|
| Corrected Model | 12,960[a] | 3 | 4.320 | 7.246 | .000 |
| Intercept | 600.000 | 1 | 600.000 | 1006.434 | .000 |
| Treatment | 12.960 | 2 | 6.480 | 10.869 | .000 |
| Observer | 0.000 | 1 | 0.000 | 0.000 | 1.000 |
| Error | 87.040 | 146 | .596 | | |
| Total | 700.000 | 150 | | | |
| Corrected Total | 100.000 | 149 | | | |

a. R Squared = ,130 (Adjusted R Squared = ,112)

Table 15: Pairwise comparison table showing that the mean differences in mean ranking scores of all treatments are significantly different from each other (α=0.05). It is shown that treatment A (500 mGy) has a significant lower mean ranking score than treatment B (50 mGy) (p=0.021) and a significant higher mean ranking score than treatment C (control) (p=0.021). Treatment B (50 mGy) has a significant higher mean ranking score than treatment C (control) (p=0.000).

Dependent Variable: Score

| (I) Treatment | | Mean Difference (I-J) | Std. Error | Sig.[b] | for Difference[b] Lower Bound | for Difference[b] Upper Bound |
|---|---|---|---|---|---|---|
| a | b | -,360* | .154 | .021 | -.665 | -.055 |
| | c | ,360* | .154 | .021 | .055 | .665 |
| b | a | ,360* | .154 | .021 | .055 | .665 |
| | c | ,720* | .154 | .000 | .415 | 1.025 |
| c | a | -,360* | .154 | .021 | -.665 | -.055 |
| | b | -,720* | .154 | .000 | -1.025 | -.415 |

Based on estimated marginal means

*. The mean difference is significant at the .05 level.

b. Adjustment for multiple comparisons: Least Significant Difference (equivalent to no

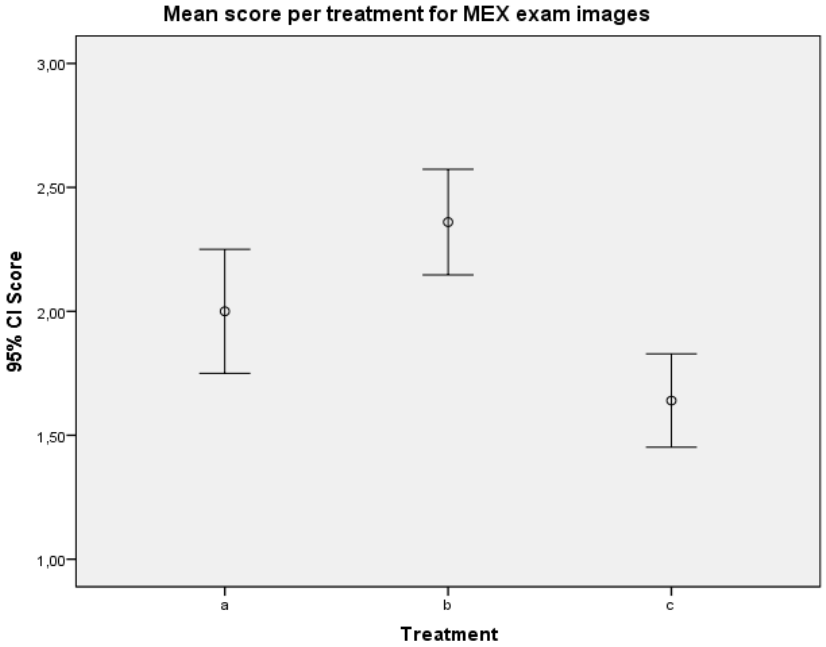


Figure 19: A visualization of the differences in mean ranking scores per treatment with their 95% confidence intervals. Treatment A is 500 mGy, treatment B is 50 mGy, and treatment C is control.

Figure 20: Biocrystallization pattern of cress extract from seedlings of which the seed batch was treated with 500 mGy Röntgen radiation.

Figure 21: Biocrystallization pattern of cress extract from seedlings of which the seed batch was treated with 50 mGy Röntgen radiation.

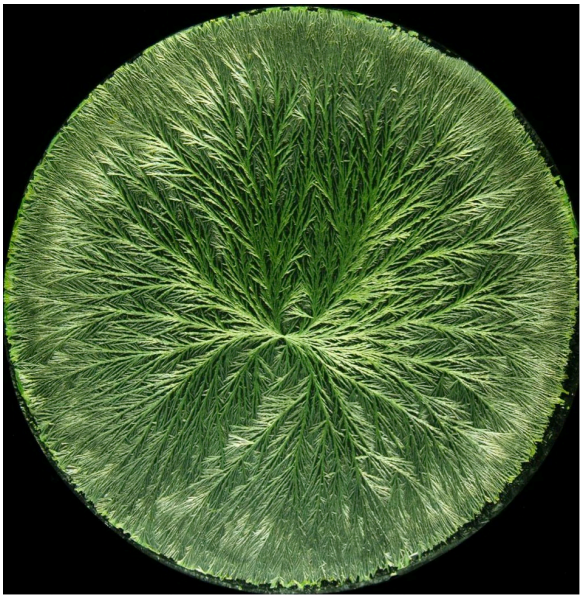

Figure 22: Biocrystallization pattern of cress extract from seedlings of which the seed batch had no Röntgen radiation treatment.

# Discussion

### Computerized image analysis examination

Computerized structure image analysis was performed on the crystallization patterns of cress extract during the experiments. The calculation of needle length fragments is executed with the analysis based on crystallization patterns of carrot extracts (Busscher, Kahl et al. 2010). An examination was performed on this analysis in order to find out whether the parameter counts for the cress extract crystallization patterns have equal distributions compared to the carrot extract crystallization patterns. It is seen that a relatively high fraction of needle fragments are located in the L≥250 region, compared to the carrot extract crystallization patterns (figure 23 and 24). For the carrot extract the computerized analysis seems to portion out its needle length fragments evenly between the selected parameters, but for the cress extract a relatively high amount of needle fragments fall under one parameter, L≥250.
The computerized structure analysis development is based on biocrystallization patterns of carrot extract, which have a coarser pattern than cress biocrystallization patterns. There is still information hidden within the L≥250 parameter from the cress extract biocrystallization patterns. This is seen from the differences in count of needle length fragments along the 15 structural analysis length-variables. So, in order for the structure image analysis to give a concrete conclusion on the needle fragment distribution, the analysis has to be improved at this point. For this, more parameters of increased needle fragment length can be included so as to subdivide the relatively large dataset of parameter L≥250.

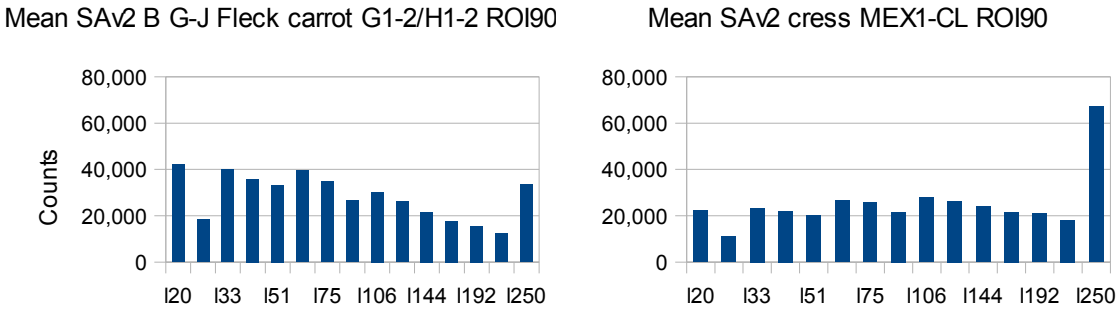


Figure 23 (left) and 24 (right): Mean filling of the 15 structural analysis length-variables for carrot biocrystallization patterns (left), versus cress-seedling biocrystallization patterns (right) at ROI 0-90%.

### Additive reference series

As a brief summary of the findings from the Additive reference series, following from the crystallization patterns of the Additive reference series the Gestalt-domain was characterized in order to become acquainted with how cress extract influences the self-organization process of $CuCl_2$. The computerized image analysis supported the findings.

The results of the performance of the chamber do not show major deviations that may be due to environmental factors in the crystallization chamber. It is thus assumed that the cause of the differences between the patterns can be explained by increasing the relative quantity of extract.
It seems that the crystallization patterns become more expressive with increasing cress extract ratio (table 5). These results were used for a Gestalt-domain characterization of 'Additive dominance' so as to observe and become acquainted with how cress extract influences the self-organization process of $CuCl_2$.
There was no ranking test performed on this reference series. The relevance of performing such a test was of minor importance, because visually the differences were quite clear.
The computerized image analysis could distinguish the treatments in terms of the needle length distribution. This supports the visual observations. However, computerized structure image analysis is based on a single morphological criterion, namely needle fragment length. These needle fragments are very hard to observe and analysed through visual evaluation, as the analysed

fragments range from 0.08 mm up to ≥0.93 mm with a total count of more than 300,000 fragments (figure 23 and 24). Visual evaluation is more based on a Gestalt-domain characterization instead of solely analysing morphological criteria. Besides, in order for the structure image analysis to give a concrete conclusion on the needle fragment distribution, the analysis has to be improved at this point. However, differences that are now observed through the computerized image analysis can be used as support for the visual evaluation results.

### Decomposition reference series

To summarize the main findings on the decomposition reference series, it was shown that the visual evaluation could significantly distinguish between the treatments, and could categorize the crystallization patterns in the right order. Computerized image analysis could support these findings, but to a certain extent.

Because the analysis of the chamber performance does not show major issues that may result in deviations among the crystal patterns, the differences within the crystallization patterns that are detected are assumed a consequence of the treatment factors.
After the Gestalt-domain 'Decomposition' was characterized, the ranking test based on visual evaluation of the patterns has shown it could differentiate between the crystallization patterns of a fresh, one day, and three days decomposed extract. Moreover, the visual evaluation could group the treatments in the right order. Computerized image analysis also could differentiate between the different treatments. However, the three days decomposed extract was different from the expected trend. During the laboratory process of making the three days and four days decomposed extract, homogenizing the extract was not performed properly, which can explain why in the computerized image analysis the distribution of the three days aged decomposed extract is not in line with the expected trend. However, with this reasoning it would be expected from the 4 days extract that it would deviate from the expected trend as well, but it did not show any peculiarities in the analysis. Within the visual evaluation it was shown that significant differences were found between the one-day decomposed extract and the three days decomposed extract crystallization patterns, while none of the depicted computerized image analysis structure parameters could differentiate between the biocrystallization patterns of 1 and 3 days decomposed extract. It can be hypothesized that this effect may be due to the lack of the computerized structure image analysis regarding parameter L≥250.
Regarding the applicability of this decomposition reference series for the Röntgen experiments, the biocrystallization patterns were already considerably affected by a one-day decomposed extract. It seems unlikely that such effects are found within the biocrystallization patterns of the Röntgen irradiated seeds. The fact that within the 3 and 4 days decomposed extract the reliability on the findings is questionable is, therefore, not of major importance concerning the Röntgen radiation experiments. From this reference series experiment it can be concluded that the characterized Gestalt-domain of 'Decomposition' can be used within the evaluation of the Röntgen radiation crystallization patterns.

### Röntgen radiation experiment

Summarizing the main results found briefly, the different treatments showed in the seedling analysis a distinction of only the 50 mGy radiated seeds exhibiting an increased root length, but root weight was not significantly higher. The seedlings of the 500 mGy radiated seeds and the seedlings of the control group are assumed to have an equal root length and weight. From the perceptual learning under supervised categorization of the crystallization patterns, it became clear that not only 'Decomposition' characteristics were apparent. A refinement was needed in order to distinguish the crystallized patterns of the different treatments from each other. This refinement included chaotic features as observed in the crystallization patterns. Within the visual evaluation the seedlings of the 50 mGy radiated seed batch was scored as having the most 'Decomposition' characteristics and having most chaotic features. The crystallization patterns of the 500 mGy radiated seed batch showed less of these characteristics, and the control group was scored as having the least 'Decomposition' characteristics and the least chaotic structures. Computerized

structure image analysis has not been able to distinguish between the distributions of needle length fragments.

***Seedling analysis***

Comparing the cress seedling analysis results with the decoding table, the 50 mGy Röntgen radiation dose led to a significant higher root length (table 10). Because root length and root weight are positively correlated with each other, root weight is influenced as well, but does not show significance. The fact that it was not significant is probably due to the number of observations within the root weight analysis (N = 75), which were considerably lower than the number of observations in the root length analysis (N = 1251) due to the followed procedure. The standard deviation from the root weight analysis was too high in order to distinguish the treatments from each other (table 11). As a consequence from the lower number of observations, the power of the statistical analysis decreases and significant differences between the treatments are thus harder to proof. Nevertheless, the mean root weight of the 50 mGy treatment has the tendency to be higher than both the 500 mGy treatment and the control group. Therefore, it is expected that significant results would be obtained when the number of root weight observations would be increased.
This result is in line with the earlier findings of growth inducing effects of relatively low-dose seed irradiation stated in Zaka et al. (2004).

***Crystallization pattern evaluation***

For the visual and computerized evaluation of the crystallization patterns, the results of the crystallization chamber performances do not show systematic deviations for any specific treatment. It is therefore assumed that differences between the biocrystallization patterns are due to the radiation treatments.
Computerized structure image analysis has not been able to distinguish between the distributions of needle length fragments (data not shown). This may be a consequence of the parameter L≥250, containing a relatively high amount of fragment count as compared to the other parameters. So, our visual evaluation results cannot be supported by the computerized structure image analysis.
It is significantly shown that within the visual evaluation there are differences between the treatments. These differences at a first glance, however, do not seem to match with the decoding table. Chaotic structures and 'Decomposition' features are most present in the crystallization patterns of the seedlings from which the seeds batch was treated with 50 mGy, whereas one would expect this would have been the most intense irradiated seed batch. However, the crystallization patterns of seedlings from which the seed batch was irriadiated with 500 mGy had a mean rank score of 2.00, significantly lower than the 50 mGy treatment (mean rank score = 2.36).
However, relating a higher degree of chaotic structural features and 'Decomposition' characteristics from the Gestalt evaluation to a higher degree of Röntgen radiation doses cannot be postulated, because there was no reference series made from known radiation doses. Consequently, a cause-effect relationship between Röntgen radiation dose and differences between crystallization structures cannot be established. The relevant features that were used to distinguish between the crystallization patterns were based on perceptual-learning according to supervised categorisation, but these features were not related to the degree of radiation doses, because the treatments were coded. The assumption was made that more 'Decomposition' features in the crystallization patterns were caused by a higher degree of radiation. However, during the perceptual-learning prior to the exam, it was shown that scoring the crystallization patterns on 'Decomposition' features only could not distinguish the treatments from each other. Instead, it was found that chaotic structures were also apparent within the crystallization patterns, and to a higher extent within the crystallization patterns of the 50 mGy treatment, albeit not systematically. It became clear that distinguishing between the treatments was more complex and could not be reduced to only one Gestalt-domain. On top of that, although the crystallization patterns were assigned to series of comparable crystallization time, the patterns still showed to some degree morphological variability making the inner sense of activity of the dynamics between the crystallization structures harder, and consequently the distinction. Still, a significant difference is observed between the treatments from the visual evaluation, and it can be stated that a higher degree of 'Decomposition' characteristics and chaotic structural features do not match with a higher degree of radiation doses. Therefore, another explanation of these results is needed.

***Hormesis***

When comparing the seedling analysis results with the visual evaluation results, it can be seen that the 50 mGy treatment shows anomalies. Within the seedling analysis the roots of the seedlings from which the seeds were irradiated with 50 mGy are systematically longer (table 10), and within the visual evaluation this treatment shows a higher degree of 'Decomposition' and chaotic features (figure 19). However, when increasing the radiation dose these results seem to decrease in effect: root length is assumed to be equal between no radiation and 500 mGy (table 12). Thereby, the found radiation effects in the crystallization patterns decrease in effect regarding the differences between the control group and 50 mGy, and the control group and 500 mGy (figure 19).

The observed results can be explained by hormesis. "Hormesis represents the advantage gained by the individual from resources initially and principally allocated for repair activities but modestly in excess of that needed to repair the immediate damage." (Calabrese and Baldwin 2002) In the case of Röntgen radiation, hormesis relates to growth inducing effects of relatively low-dose irradiation but showing growth-inhibiting effects of higher doses (Sagan 1987) by radiation-induced apoptosis and terminal cell differentiation (Feinendegen 2005). The so-called beneficial effects of the relatively low radiation dose in the mGy range result from adaptive protection against DNA damage from many, mainly endogenous, sources, depending on cell type, species and metabolism (Feinendegen 2005). These effects decrease steadily above a dose of 100 mGy to 200 mGy and are not observed anymore above 500 mGy (Feinendegen 2005). Such growth-inducing effects are more generally seen as overcompensating effects due to a temporal disruption in homeostasis (Calabrese and Baldwin 2002).

The results of the visual evaluation show a higher degree of 'Decomposition' characteristics and chaotic structural features within a low-dose Röntgen radiation treatment of 50 mGy. From what is known from earlier findings on the effects of low-dose Röntgen radiation it can be hypothesized (1) that the increase in 'Decomposition' characteristics and chaotic structural features of the crystallization patterns of the 50 mGy treated seeds is the result of a disruption in homeostasis. This induces a hormetic response, which is an organismal strategy for optimal resource allocation through inducing agonist concentration gradients to ensure homeostasis is maintained (Calabrese and Baldwin 2002). However, overcompensation is the consequence. This results in e.g. higher root length growth, which is confirmed by the cress seedling analysis. From the seedling analysis only one could conclude low-dose seed irradiation shows indeed a beneficial response, as is stated in earlier scientific research reports (Zaka, Chenal et al. 2004). However, such judgemental characterization is not generally useful, even can be described as overly simplistic, as the underlying mechanism is more complex (Calabrese and Baldwin 2002). Because, what is observed in the crystallization patterns is that actually a disruption may be seen in homeostasis, hence a more harmful effect than a beneficial effect.

A second hypothesis (2) is that this result is not observed in the crystallization patterns of the 500 mGy treated seeds, because the cress seeds had had a Röntgen radiation dose outside of the region in which agonist concentration gradients are induced as a consequence of a disruption in homeostasis (Calabrese and Baldwin 2002). Consequently, an adaptive response is not initiated, which is also confirmed by the seedling analysis.

At last (3), increasing the radiation dose beyond 500 mGy would have toxic effects as mentioned in Feinendegen (2005) like apoptosis and terminal cell differentiation, and would therefore decrease root length. But how increased Röntgen radiation doses will influence the crystallization pattern formation cannot yet be stated from these results and a reference series based on increasing radiation doses is therefore needed. Within the context of evaluating the effects of Röntgen radiation detection analysis, however, it seems not to make sense to carry out such a reference series, because such high levels are not allowed within detection purposes. However, in order to have a more founded base on the effects of Röntgen radiation on physiological processes shown in the crystallization patterns, such a reference series could give more insight.

***Crystallization pattern formation***

It is still being investigated how physiological processes of a sample prior to crystallization influence the pattern formation exactly (Busscher, Kahl et al. 2014). From a thermodynamic point of view, crystallization pattern formation is the process of fixing randomly moving molecules by passing on the energy of their movement to the liquid in which they are dissolved. So, the liquid effectively increases in entropy and the crystal itself decreases in entropy (Heylighen 2001). It is assumed that a more processed juice or extract has a higher entropy (Busscher, Kahl et al. 2014). This means that the molecules in the solution have a higher randomization. The question then to be solved is how randomization of molecules affects the process of fixation of the molecules in the solution or, in other words, the crystallization pattern formation.

Due to this lack of knowledge, a direct link between the observed patterns and physiological perturbations, in this case Röntgen radiation cannot yet be established. In addition, the biocrystallization method uses a solution of dihydrate cupric chloride that self-organizes into crystallization patterns under standardized procedures. An extract is then added, but only affects the self-organization process of cupric chloride. The self-organization of the extract is not directly shown in the crystallization pattern. Consequently, it cannot be stated that the emerged crystallization patterns reflect the self-organization processes of the extract. However, although a direct link between the crystallization pattern and the treated extract cannot be made, the results show that crystallization patterns between treatments can be distinguished significantly. Therefore, it is assumed that the differences between the crystallization patterns reflect underlying physiological mechanisms.

The results of these experiments can be explained through hormesis, which seems to be a plausible explanation. Further understanding of the process of crystallization is needed before drawing conclusions directly via the crystallization patterns. The importance of understanding this method is already mentioned by Kahl et al. (2010) in relation to food authentication. Besides, the entropy exporting process that underlies the pattern formation is a process that occurs in all living organisms (Heylighen 2001): "Plants and animals take in energy and matter in a low entropy form as light or food. They export it back in a high entropy form, as waste products. This allows them to reduce their internal entropy." Entropy exporting is an aspect of maintaining homeostasis of an organism, in other words keeping the organism away from thermodynamic equilibrium.

***Self-organization and homeostasis***

Moreover, this process is not only applicable within individual organisms. "We suggest that life exists on earth as another means of dissipating the solar induced gradient and, as such, is a manifestation of the restated second law of thermodynamics." (Schneider and Kay 1995) The process of reducing gradients, or dissipation, is manifested through the process of self-organization, and this is applicable to all living systems on earth. In addition, dissipative processes in living systems can continue without the dependency on stochastic events. This is achieved by regulatory mechanisms like DNA, which is seen as a memory agent that allows maintenance of the dissipative structures (Schneider and Kay 1995). Just like DNA, other regulatory mechanisms have evolved in order to maintain dissipative structures. In agriculture such regulatory mechanisms gain more and more attention (Napel ten, Bianchi et al. 2006). Furthermore, the more regulation processes, the higher the resilience of a system, the harder it is for a perturbation to switch the system to an alternative state (Scheffer, Carpenter et al. 2001). However, without any perturbations a system may end up in a local stable state, but having the potential to reach a stable state even further from thermodynamic equilibrium. Perturbations in a system can disturb a system such that it has the possibility to switch to an alternative stable state (Scheffer, Carpenter et al. 2001). However, this alternative stable state can be either further away from or closer to thermodynamic equilibrium (Heylighen 2001). Consequently, there should be a balance between regulatory mechanisms in order to maintain its homeostasis, and perturbations that disturb the system (Heylighen 2001).

When a system gets disturbed, regulatory mechanisms will be activated in order to maintain its homeostasis (Calabrese and Baldwin 2002). This accounts for living systems as well as individual organisms. But in order to directly analyse how homeostasis of living organisms is affected by physiological processes as a result of perturbations in its environment, a method is needed that can actually analyse such effects. Such a method would be based on a more holistic level, as it

focuses not on the regulatory mechanisms of the system, but on how the system as a whole is influenced, and reacts.
The biocrystallization method is such a holistic method (Kahl, van der Burgt et al. 2010) and shows in this experiment that the results of Röntgen radiation on cress seed complement earlier scientific findings on the effects of Röntgen radiation on homeostasis. The biocrystallization method imbues the quantitative root length analysis with a qualitative dimension. A relatively high accuracy was thereby obtained, as all visual evaluation ranking scores of the treatments were significantly different. The untreated sample was identified correctly, and the other results could be explained by hormetic effects.
Such effects cannot yet be directly concluded from the crystallization patterns. Further understanding of the crystallization pattern formation should be aimed for. The underlying mechanism behind pattern formation is self-organization, which makes dissipation of the temperature gradient possible (Schneider and Kay 1995). Studying whether plant physiological specific self-organization structures appear by observing the infrared spectra during heat convection in the dish could gain a better understanding of the pattern formation.

# Conclusion

The goal of this research project was to analyse whether radiation, as used in Röntgen detection analysis, has an effect on germinating cress seeds (*Lepidium sativum* L.) by using the biocrystallization method. The biocrystallization method imbued the quantitative root length analysis with a qualitative dimension through the ontological holistic stance of this method. It was shown that the method could correctly identify the untreated sample, and the results of the Röntgen radiated samples complemented earlier scientific findings on the effects of Röntgen radiation levels on homeostasis. From the visual evaluation of the biocrystallization patterns and the seedling analysis it is hypothesized that (1) the increase in 'Decomposition' characteristics and chaotic structural features of the crystallization patterns of the 50 mGy treated seeds is the result of a disruption in homeostasis. (2) This result is not observed in the crystallization patterns of the 500 mGy treated seeds, because the cress seeds had had a Röntgen radiation dose outside of the region in which agonist concentration gradients are induced as a consequence of a disruption in homeostasis. Finally (3), increasing the radiation dose would have toxic effects like apoptosis and terminal cell differentiation, and would therefore decrease root growth. But how higher Röntgen radiation doses will influence the crystallization pattern formation cannot yet be stated from these results.

Further understanding of the crystallization pattern formation should be aimed for. Studying whether plant physiological specific self-organization structures appear by observing the infrared spectra during heat convection in the dish could gain a better understanding of the pattern formation.

# Literature references


Andersen, J. O., C. B. Henriksen, J. Laursen and A. A. Nielsen (1999). "Computerised image analysis of biocrystallograms originating from agricultural products." Computers and Electronics in Agriculture **22**(1): 51-69.

Ashby, E. G. and W. T. Maddox (2005). "Human category learning." Annual Review of Psychology **56**: 149-178.

Baars, E. and T. Baars (2007). "Towards a philosophical underpinning of the holistic concept of integrity of organisms within organic agriculture." Njas-Wageningen Journal of Life Sciences **54**(4): 463-477.

Baumgartner, S., P. Doesburg, C. Scherr and J. O. Andersen (2012). "Development of a Biocrystallization Assay for Examining Effects of Homeopathic Preparations Using Cress Seedlings." Evidence-Based Complementary and Alternative Medicine.

Busscher, N., J. Kahl, P. Doesburg, G. Mergardt and A. Ploeger (2010). "Evaporation influences on the crystallization of an aqueous dihydrate cupric chloride solution with additives." Journal of Colloid and Interface Science **344**(2): 556-562.

Busscher, N., J. Kahl and A. Ploeger (2014). "From needles to pattern in food quality determination." Journal of the Science of Food and Agriculture.

Calabrese, E. J. and L. A. Baldwin (2002). "Defining hormesis." Human & Experimental Toxicology **21**(2): 91-97.

CollinsEnglishDictionary (2014). Harper Collins Publisher.

Doesburg, P. and A. F. M. Nierop (2013). "Development of a structure analysis algorithm on structures from CuCl2 center dot 2H(2)O crystallization with agricultural products." Computers and Electronics in Agriculture **90**: 63-67.

Feinendegen, L. E. (2005). "Evidence for beneficial low level radiation effects and radiation hormesis." British Journal of Radiology **78**(925): 3-7.

Fritz, J., M. Athmann, T. Kautz and U. Kopke (2011). "Grouping and classification of wheat from organic and conventional production systems by combining three image forming methods." Biological Agriculture & Horticulture **27**(3-4): 320-336.

Galotti, K. M. (2013). Cognitive psychology in and out of the laboratory.

Heylighen, F. (2001). The science of self-organization and adaptivity. The encyclopedia of life support systems. **5:** 253-280.

Huber, M., J. O. Andersen, J. Kahl, N. Busscher, P. Doesburg, G. Mergardt, S. Kretschmer, A. Zalecka, A. Meelursarn, A. Ploeger, D. Nierop, L. van de Vijver and E. Baars (2010). "Standardization and Validation of the Visual Evaluation of Biocrystallizations." Biological Agriculture & Horticulture **27**(1): 25-40.

Huber, M. A. S., J. Bloksma, G. J. Burgt van der and L. P. L. Vijver van de (2006). Challenges for an organic food quality concept: the Inner Quality Concept Requirements demonstrated on an experimental concept. Joint Organic Congress. Odense, Denmark.

Kahl, J., M. Bodroza-Solarov, N. Busscher, J. Hajslova, W. Kneifel, M. O. Kokornaczyk, S. van Ruth, V. Schulzova and P. Stolz (2013). "Status quo and future research challenges on organic food quality determination with focus on laboratory methods." J Sci Food Agric.

Kahl, J., G. J. van der Burgt, D. Kusche, S. Bugel, N. Busscher, E. Hallmann, U. Kretzschmar, A. Ploeger, E. Rembialkowska and M. Huber (2010). "Organic FOOD CLAIMS in Europe." Food Technology **64**(3): 38-46.
Lammerts van Bueren, E. T., P. C. Struik and E. Jacobsen (2002). "Ecological concepts in organic farming and their consequences for an organic crop ideotype." Netherlands Journal of Agricultural Science **50**: 1-26.

Lobet, G., L. Pages and X. Draye (2011). "A Novel Image-Analysis Toolbox Enabling Quantitative Analysis of Root System Architecture." Plant Physiology **157**(1): 29-39.

LomaSystems. (2013). "Guide to X-ray Inspection." Retrieved March 13, 2014, from http://www.loma.com/LOMA2013/documents/guides/Loma_Guide_to_X-ray_Inspection.pdf.

Looijen, R. C. (2000). Holism and reductionism in biology and ecology : the mutual dependence of higher and lower level research programmes. Dordrecht ; Boston, Kluwer Academic Publishers.

Napel ten, J., F. Bianchi and M. Bestman (2006). "Utilising Intrinsic Robustness in Agricultural Production Systems." Inventions for a Sustainable Development of Agriculture: 32-54.

Northolt, M., G. J. Burgt van der, T. Buisman and A. Bogaerde van den (2004). "Parameters for Carrot Quality and the development of the Inner Quality concept." Louis Bolk Instituut.

Sagan, L. A. (1987). "What Is Hormesis and Why Havent We Heard About It Before." Health Physics **52**(5): 521-525.

Scheffer, M., S. Carpenter, J. A. Foley, C. Folke and B. Walker (2001). "Catastrophic shifts in ecosystems." Nature **413**(6856): 591-596.

Schneider, E. E. and J. J. Kay (1995). "Life as a Manifestation of the Second Law of Thermodynamics." Mathematical and computer modelling **19**(6): 25-48.

Tscharntke, T., R. Bommarco, Y. Clough, T. O. Crist, D. Kleijn, T. A. Rand, J. M. Tylianakis, S. van Nouhuys and S. Vidal (2007). "Conservation biological control and enemy diversity on a landscape scale." Biological Control **43**(3): 294-309.

Zaka, R., C. Chenal and M. T. Misset (2004). "Effects of low doses of short-term gamma irradiation on growth and development through two generations of Pisum sativum." Science of the Total Environment **320**(2-3): 121-129.

# Attachments

**1. Examples of seedlings in bag per treatment**

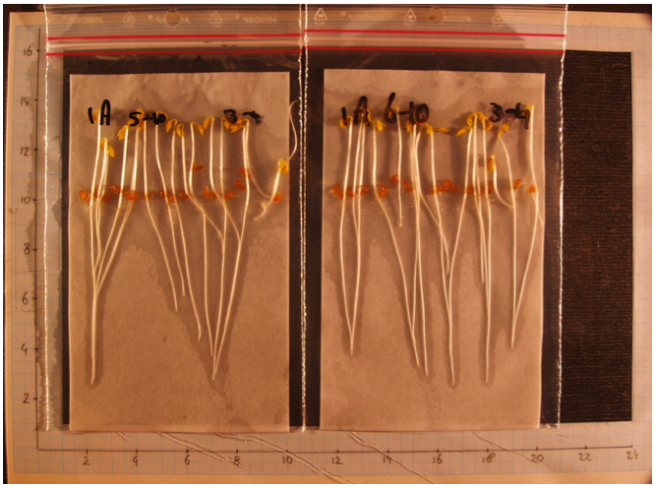

Figure 25: Example of seedlings after 96 h of germination, treatment A (500 mGy), bag replicate 5 and 6, first experiment (3rd of April).

Figure 26: Example of seedlings after 96 h of germination, treatment B (50 mGy), bag replicate 1 and 2, second experiment (10th of April).

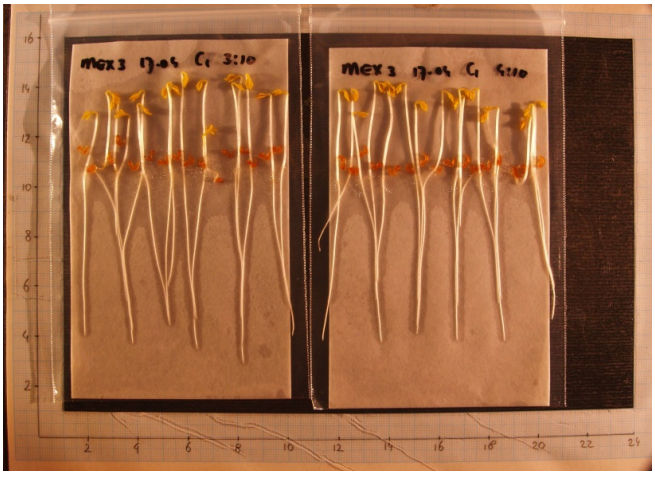

Figure 27: Example of seedlings after 96 h of germination, treatment C (control), bag replicate 3 and 4, third experiment (17th of April).

## 2. General set-up Additive reference series experiment

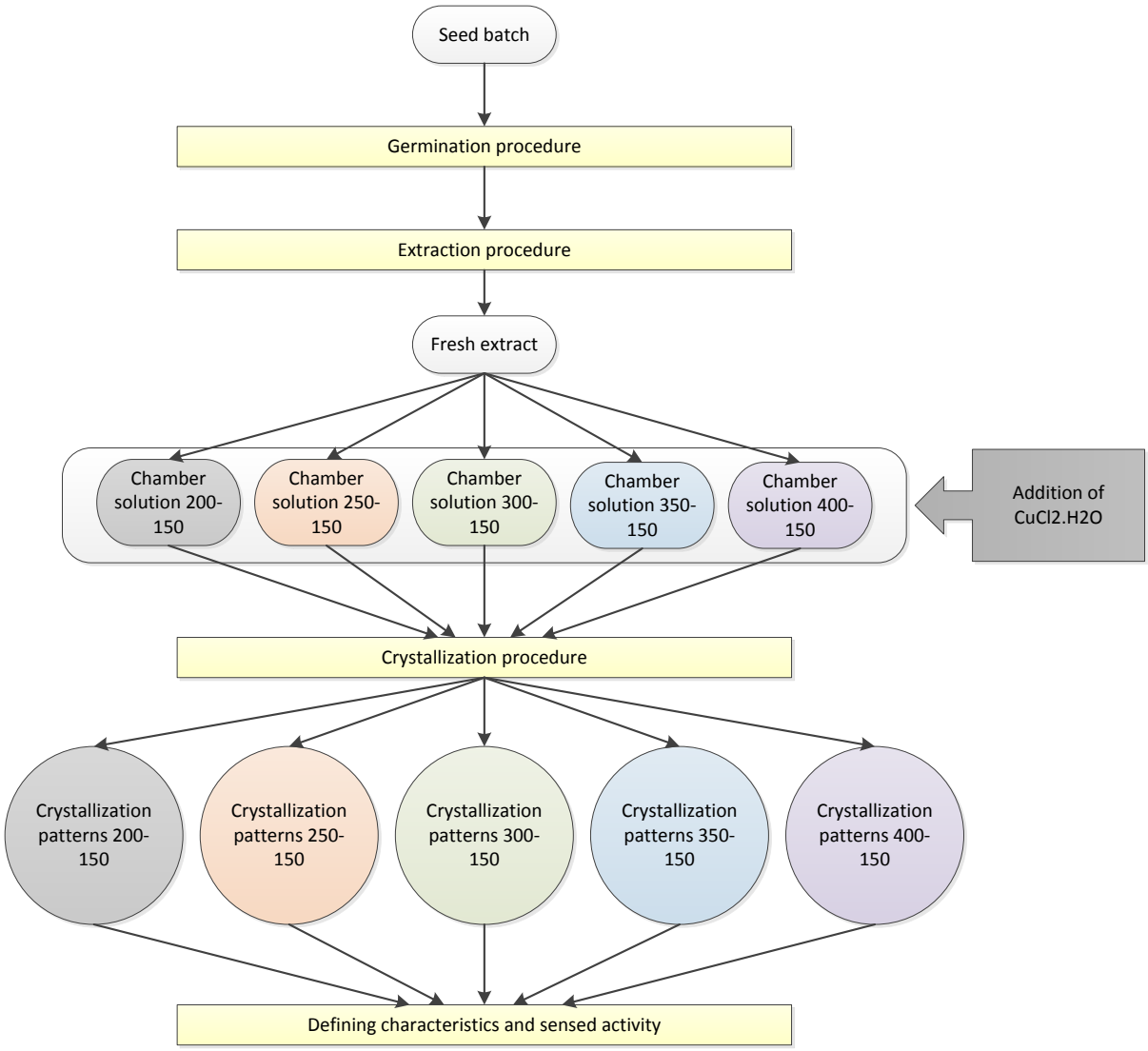

## 3. General set-up Decomposition reference series experiment

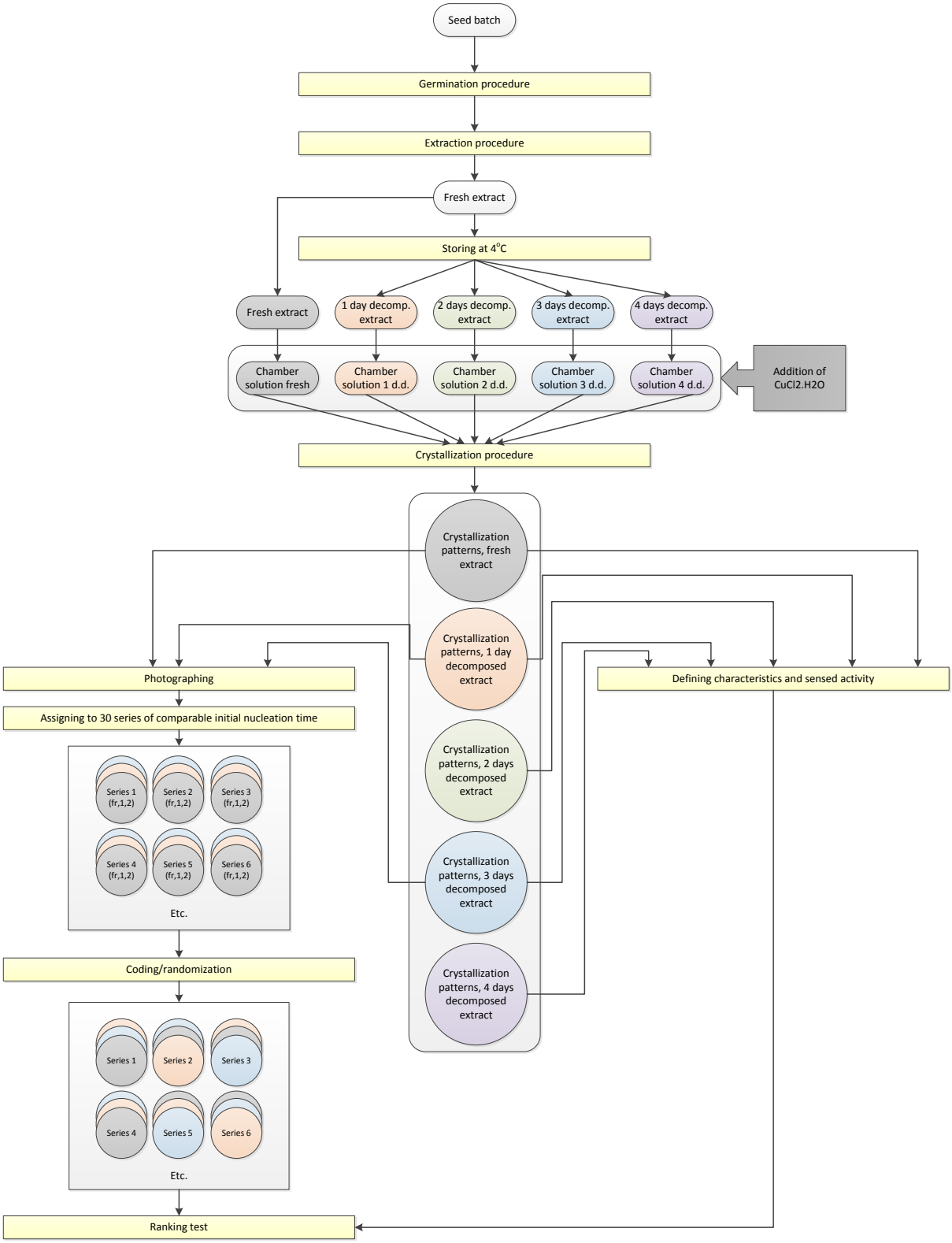

## 4. General set-up Röntgen radiation experiment